THE JOURNAL OF BIOLOGICAL CHEMISTRY
Vol. 275, No. 3, Issue of January 21, pp. 2165–2173, 2000

Printed in U.S.A.

Determinants of the Peptide-induced Conformational Change in the Human Class II Major Histocompatibility Complex Protein HLA-DR1*

(Received for publication, September 23, 1999, and in revised form, October 28, 1999)

Aaron K. Sato‡§, Jennifer A. Zarutskie‡§, Mia M. Rushe¶, Aleksey Lomakin¶, Sateesh K. Natarajan‖, Scheherazade Sadegh-Nasseri‖, George B. Benedek¶, and Lawrence J. Stern‡**

From the Departments of ‡Chemistry and ¶Physics, Massachusetts Institute of Technology, Cambridge, Massachusetts 02139 and the ‖Department of Pathology, Johns Hopkins University School of Medicine, Baltimore, Maryland 21205

The human class II major histocompatibility complex protein HLA-DR1 has been shown previously to undergo a distinct conformational change from an open to a compact form upon binding peptide. To investigate the role of peptide in triggering the conformational change, the minimal requirements for inducing the compact conformation were determined. Peptides as short as two and four residues, which occupy only a small fraction of the peptide-binding cleft, were able to induce the conformational change. A mutant HLA-DR1 protein with a substitution in the β subunit designed to fill the P1 pocket from within the protein (Gly^{86} to Tyr) adopted to a large extent the compact, peptide-bound conformation. Interactions important in stabilizing the compact conformation are shown to be distinct from those responsible for high affinity binding or for stabilization of the complex against thermal denaturation. The results suggest that occupancy of the P1 pocket is responsible for partial conversion to the compact form but that both side chain and main chain interactions contribute to the full conformational change. The implications of the conformational change to intracellular antigen loading and presentation are discussed.

Class II major histocompatibility complex (MHC)[1] proteins bind peptide antigens and present them to $CD4^+$ T-cells, a process crucial to T-cell selection and initiation of T-cell-mediated immune responses (1, 2). They are cell surface glycoproteins composed of highly polymorphic α and β subunits (~30,000 molecular weight for each subunit), in complex with one bound peptide/molecule. The peptide binding site is found on the substantial extracellular portion of the protein and is formed by both α and β subunits (3); in addition, each subunit has one transmembrane span and a small cytoplasmic portion. Three-dimensional structures have been determined for peptide complexes of extracellular domains of several human (HLA-DR) and murine (I-A and I-E) class II MHC proteins (4–10). In each of the structures, the peptide is bound in an essentially identical extended conformation, similar to a polyproline II-helix or a twisted β strand, with the conformation apparently maintained by a large number of interactions between the peptide main chain and the MHC protein (10, 11). Side chains of the bound peptides project into allele-specific pockets within the overall peptide-binding site.

The peptide binding specificities of class II MHC proteins from human, mouse, and other species have been extensively studied (12). Endogenous peptides isolated from class II MHC molecules expressed by antigen presenting cells generally have lengths ranging from 15 to 20 residues, with longer peptides found occasionally (13–15). Class II MHC proteins generally recognize amino acid side chains embedded within a ~9-residue stretch of a bound peptide. Within this binding frame, there are relatively strong side chain preferences at several positions and relatively weaker preferences at others. Sequences outside the binding frame have little or no effect on peptide binding specificity. This pattern of side chain preferences, called the peptide-binding motif, is consistent with the x-ray crystal structures, which reveal pockets in the peptide-binding site spaced to accommodate the peptide side chains that contribute to the motif. The pockets are labeled according to the side chain accommodated; for example, the P1 pocket binds the side chain of the residue in the +1 position. In the structures of HLA-DR alleles, pockets within the overall peptide-binding site are at P1, P4, P6, and P9, with smaller pockets or shelves in the binding site at P3 and P7 (see Fig. 1) (3, 7, 8, 10, 16). Initial descriptions of the peptide-binding motifs of HLA-DR alleles indicated preferences only at these positions, with the P1 position having the greatest effect (17, 18). More sophisticated recent characterizations of the motif include also the effect of positive and negative contributions of each amino acid at all positions within the binding frame, with the motifs described by full 20 (side chain) × 9 (position) matrices (19). For other MHC proteins the pattern of side chain and length preferences is very similar, except that several HLA-DQ and murine I-A alleles have reduced or absent side chain preferences at the P1 position (4, 6). The relative contributions of peptide side chain and main chain interactions to the MHC class II binding affinity and complex stability have not been addressed in detail.

Several recent studies have suggested that class II MHC proteins can adopt alternate conformations under certain experimental conditions or when peptide binding is absent or destabilized. (20–26). The first observations of conformational variation in class II MHC were the presence of an intermediate "floppy" species with reduced mobility on nondenaturing SDS-

* This work was supported by National Institutes of Health Grants R01-AI38996 (to L. J. S.), P01-GM56552 (to L. J. S.), and R01-GM53549 (to S. S. N.), Council for Tobacco Research Grant 4314 (to S. S. N.), and a Merck predoctoral fellowship (to J. A. Z). The costs of publication of this article were defrayed in part by the payment of page charges. This article must therefore be hereby marked "*advertisement*" in accordance with 18 U.S.C. Section 1734 solely to indicate this fact.

§ These authors contributed equally to this work.

** To whom correspondence should be addressed: Dept. of Chemistry, Massachusetts Institute of Technology, 77 Massachusetts Ave., Cambridge, MA 02139. E-mail: stern@mit.edu.

[1] The abbreviations used are: MHC, major histocompatibility complex; PBS, phosphate-buffered saline; PAGE, polyacrylamide gel electrophoresis.

PAGE during thermal denaturation and folding (27, 28). This floppy species was the predominant species at low pH (29). Such conformational changes have been proposed to play important roles in the peptide binding process *in vivo* and in interactions with other proteins, such as the peptide exchange factor HLA-DM (20, 22, 30, 31). For HLA-DR1 (*DRA*0101* and *DRB1*0101*), a common human class II MHC protein, we have shown that peptide binding drives conversion between two defined states, a looser, more open conformation for the empty protein, and a compact conformation for the peptide-bound form (21, 26). The conversion involved a decrease of the hydrodynamic radius from ~35 to ~29 Å, an alteration in secondary structure, and an increase in the cooperativity of thermal denaturation. Together these results suggested a condensation or folding of the empty protein around the peptide. In this work, we investigate the minimal determinants of the peptide-MHC interaction needed to trigger the conversion to the compact form. We find that the peptide length and sequence requirements for inducing the conformational change are distinct from those for tight binding and in particular that occupancy of the P1 pocket is sufficient for transition to a compact form.

EXPERIMENTAL PROCEDURES

HLA-DR1 Expression and Folding—The extracellular portion of HLA-DR1 (α1–188, β1–194) was produced by expression of individual subunits in *Escherichia coli* inclusion bodies followed by refolding the subunits together *in vitro* as described (32). For production of the mutant $DR1_{\beta G86Y}$, with glycine at position β86 replaced by tyrosine, a recombinant β subunit expression plasmid was constructed by replacing the *Afl*III-*Bsp*EI fragment of the native gene with one from a recombinant baculovirus vector carrying the mutation (33). Briefly, HLA-DR1 subunits were isolated from inclusion bodies by ion exchange chromatography in 8 M urea containing 1 mM dithiothreitol and were folded together by dilution into 10% glycerol containing pH and redox buffers (32). Folded empty HLA-DR1 and $DR1_{G\beta 86Y}$ proteins were recovered by immunoaffinity chromatography using a conformation-specific monoclonal antibody (LB3.1) and were transferred into PBS (136 mM NaCl, 3 mM KCl, 10 mM Na_2HPO_4, 2 mM KH_2PO_4, 0.02% NaN_3, pH 7.2). For long term storage at 4 °C, 10% glycerol was added and was removed by spin ultrafiltration (Amicon-10) before analysis (21).

Peptide Complexes of HLA-DR1—Peptides were synthesized using solid phase Fmoc (*N*-(9-fluorenyl)methoxycarbonyl) chemistry, deprotected, and purified by reverse phase chromatography using standard methods. Peptides bHa and bHa_{Y308A} were biotinylated at their terminal amine groups using LC-LC-biotin succinimide ester (Pierce), where LC corresponds to a 6-aminohexanoic acid linker, before side chain deprotection and cleavage from the synthesis resin. The identity of the purified peptides was confirmed by matrix-assisted laser desorption mass spectrometry. Peptide complexes were prepared by incubating purified empty HLA-DR1 (1–5 μM) with at least 5-fold molar excess peptide for 3 days at 37 °C in PBS (34). Alternately, tightly binding peptide complexes (Ha and Yak; $K_D < 100$ nM) were produced by folding subunits in the presence of excess peptide with purification by immunoaffinity chromatography as described above. The extent of peptide binding was routinely assayed by 10% native PAGE or by 12.5% SDS-PAGE with samples boiled or not in loading buffer containing 1% SDS before loading. The peptide-DR1 complexes were further purified by gel filtration or ion exchange to remove aggregates and unbound peptide. The concentration of HLA-DR1 and peptide complexes was measured by UV absorbance at 280 nm using ϵ_{280} of 54,375 M^{-1} cm^{-1} for the wild-type protein. The extinction coefficient was adjusted for the Gly → Tyr substitution and for the presence of peptide tyrosine using $\epsilon_{280,\,Tyr}$ of 1280 M^{-1} cm^{-1}. Complexes of weakly binding peptides ($K_D < 1$ μM) were maintained in the presence of at least 50 μM excess peptide for further characterization.

K_D Determinations—For biotinylated peptides bHa and bHa_{Y308A}, dissociation constants K_D were determined using a direct binding assay. A fixed concentration of empty HLA-DR1 or $HLA\text{-}DR1_{G\beta 86Y}$ (0.5 nM) was mixed with varying concentrations of biotinylated peptide (10^{-12}–10^{-4} M) in PBS containing 0.05% Triton X-100 and 0.3% bovine serum albumin. These mixtures were incubated at 37 °C for 3 days, followed by sandwich fluorescence immunoassay using an immobilized DR1-binding antibody (LB3.1) and soluble Eu-labeled streptavidin. A 96-well polystyrene microtiter plate (Dynex Immulon 4) was prepared by adding LB3.1 (10 μg/ml in PBS) to each well. Following incubation at 37 °C for 1 h, the plate was blocked with PBS containing 3% bovine serum albumin at 37 °C for 1 h. After incubating the samples with the plate at 37 °C for 30 min, the plate was washed again, and streptavidin-Eu (Wallac, 1:1000 in DELFIA™ assay buffer) was applied to each well. Following incubation at 37 °C for 15 min, the plate was washed, and bound Eu was detected using a fluorescence-enhancing chelator solution (DELFIA enhancement solution) and a Wallac VICTOR™ 1420 Multilabel Counter. Plots of bound fluorescence *versus* peptide concentration were fit to a binding quadratic. The K_D for the complex of wild-type HLA-DR1 and bHa was 14 nM, similar to a previously reported value (13 nM) for ^{125}I-Ha (35). The K_D for the $HLA\text{-}DR1_{\beta G86Y}$ and bHa_{Y308A} complex was 9 μM.

For other peptides, relative binding affinities were determined by a competition assay, essentially as described (36). Empty HLA-DR1 (0.5 nM) was mixed with a fixed concentration of biotinylated probe peptide (0.5 nM bHa for HLA-DR1 or bHa_{Y308A} for $HLA\text{-}DR1_{\beta G86Y}$) and varying concentrations of unlabeled competitor peptides (10^{-10} to 10^{-3} M). The mixtures were incubated at 37 °C for 3 days, followed by detection of bound biotinylated peptide using the solid phase immunoassay described above. IC_{50} values were obtained from the best fit line of the competitive binding equation to plots of fluorescence *versus* concentration of competitor peptide and were converted to K_D values using the equation, $K_D = (IC_{50})/(1+([bHa]/K_{D,\,bHa}))$.

Gel Filtration—A Superdex 200 HR gel filtration column (Amersham Pharmacia Biotech) run at 0.3 ml/min in PBS (pH 6.8) was calibrated using thyroglobulin (670 kDa), γ-globulin (158 kDa), ovalbumin (44 kDa), and myoglobin (17 kDa) (Bio-Rad). Apparent molecular masses of empty and peptide-loaded DR1 were estimated from their respective elution volumes by reference to calibration plots (37). Confidence intervals reported in Table I reflect both the standard deviation from the mean elution volume for replicate samples and the uncertainty in the nonlinear least squares fit to the calibration plot.

Determination of Hydrodynamic Radius by Dynamic Light Scattering—Samples were prepared for dynamic light scattering by exchange into PBS and concentrated by centrifugal ultrafiltration (0.1–1 mg/ml). The samples were centrifuged at 5000 rpm for 30 min to remove dust. Pilot experiments confirmed that there is no concentration dependence of the hydrodynamic radius in this concentration range. Dynamic light scattering measurements were made at 25 °C with an argon ion laser (Coherent Innova 90, 25 W, $\lambda = 488$ nm) at a scattering angle of $\theta = 90°$ and were converted to diffusion coefficient distributions using an autocorrelation function as described previously (21, 38). The distribution of diffusion coefficients was converted into a distribution of hydrated radius R_{hydr} using the Stokes-Einstein equation (39) as described previously (21). Confidence limits for these measurements reflect the standard deviation from the mean of the replicate measurements and uncertainty in temperature.

Circular Dichroism Spectroscopy and Thermal Stability—For CD analysis, purified empty DR1 and DR1-peptide complexes (0.2–0.6 mg/ml) were exchanged by dialysis into 10 mM sodium phosphate buffer, pH 7.0, and filtered through a 0.45-μm filter. Low affinity complexes were maintained in solutions containing excess peptide, with a blank solution containing the same concentration of peptide used as a background control. CD measurements were made at 4 °C in a cell with a 1-mm path length as described (32), with dichroism reported on a per residue basis. Thermal denaturations were performed as described (32), monitoring the change with temperature of the CD signal at 204 nm, which is near a negative peak in the native minus denatured difference spectrum. Thermal denaturation data were interpreted using a seven-parameter function that describes a two-state transition (40, 41).

$$\theta = (\theta_u + muT) + \left[\frac{(\theta_f - \theta_u) + T(mf - mu)}{1 + \exp - \left[\frac{\Delta H}{RT} + \frac{\Delta C_p}{R}\left(\frac{T_m}{T} - 1 + \ln\frac{T}{T_m}\right)\right]}\right] \quad \text{(Eq. 1)}$$

For reasonable values of the apparent heat capacity change, ΔC_p (10–3000 kcal mol^{-1} K^{-1}), no dependence of the parameters on the value of ΔC_p is observed. Therefore, a fixed value of $\Delta C_p = 1000$ kcal mol^{-1} K^{-1} was used to fit the parameters T_m (the midpoint denaturation temperature), ΔH (the apparent van't Hoff denaturation enthalpy), θf and mf (the y intercept and slope of a line describing the folded protein dichroism), and θu and mu (the corresponding values for the unfolded protein dichroism). T_m values were verified by first derivative analysis. ΔH uncertainties represent only the fit of the data to the equation shown above and not uncertainty in the two-state approximation. Although the melting transitions are accompanied by irreversible denaturation,

at the scan rates used (1 °C/min) thermodynamic parameters reflect the underlying unfolding process (21, 42).

KL-295 Antibody Reactivity—Antibody binding specificity was measured using a sandwich enzyme-linked immunosorbent assay as described previously (21). Monoclonal antibody KL-295 (43) was used at 10 μg/ml to coat a 96-well polystyrene microtiter plate by incubation overnight at 4 °C. The plate was blocked with 3% bovine serum albumin in PBS and washed with PBS containing 0.05% Triton X-100 (PBST). Quadruplicate 2-fold dilutions of empty DR1 or peptide complexes (1–300 nM) in PBST were added, allowed to bind to the plate for 30 min at 37 °C, and washed with PBST. For YR, Min4, and Phen7 samples, 100 μM free peptide was added to the incubations to prevent bound peptide dissociation. The amount of bound DR1 was detected ($A_{405\ nm}$) by sequential incubations with rabbit anti-DR polyclonal antibody, goat anti-rabbit peroxidase conjugate, and 2,2-azino-di-[3-ethylbenzathiazoline sulfonate] as described (34).

RESULTS

Design and Construction of Complexes of HLA-DR1 with Analogues of the Ha Peptide—To investigate roles played by different regions of the peptide ligand in triggering the HLA-DR1 conformational change, we used several analogues of the tightly binding peptide Ha derived from influenza hemagglutinin (Fig. 1) (10, 35). Peptides Ha_{Y308A} and Yak were designed to investigate the role of interactions between peptide side chains and MHC side chain-binding pockets (44). These are full-length analogues (13 residues) with an alanine substitution for the tyrosine at P1 (Ha_{Y308A}) or with alanine substitutions at all of the positions except the P1 tyrosine and the P8 lysine, which was retained for solubility (Yak) (Fig. 1). The P8 side chain does not contact the MHC protein (7, 10). These peptides were used in an earlier study demonstrating the key importance of interactions in the P1 site to the overall binding affinity (44). Peptides Phen7, Min4, and YR are shorter peptides designed to investigate the peptide length dependence of the conformational change. Peptide Phen7 retains interactions in the P1–P7 region, with favorable but not optimal side chains at P1 and P6 (Fig. 1) (17, 18, 44). The shorter peptide Min4 has optimal side chains at every position (18) and retains interactions in the P1-P4 region only (Fig. 1). The dipeptide YR has optimal side chains at both P1 and P2 positions. Peptides Phen7, Min4, and YR all carry N-terminal acetyl and C-terminal amide groups to prevent potential complications from introduction of charged residues in the site. Peptide complexes were prepared by binding the peptide of interest to empty HLA-DR1 refolded *in vitro* from subunits expressed in *E. coli* inclusion bodies (32).

Binding affinities of analogue peptides were determined by a competition immunoassay using biotinylated Ha (bHa) (see "Experimental Procedures" for details). Half-maximal inhibitory concentrations were converted to binding affinities using the known K_D for bHa, which was determined in a direct binding assay to be 14 nM (Fig. 2*A*). Peptide Yak bound to HLA-DR1 with high affinity, although more weakly than the parent Ha peptide (Fig. 2*B* and Table I). This indicates that large side chains at positions other than P1 do not play a controlling role in determining the binding affinity. However, single substitution of the P1 tyrosine by alanine in the Ha_{Y308A} peptide caused a large decrease in binding affinity, with Ha_{Y308A} binding more than 1000-fold worse than the parent Ha peptide (Fig. 2*B* and Table I). This substantiates the key role of the P1 residue in binding to HLA-DR1, as previously observed (44–46). The shorter peptides Phen7 and Min4 both bound substantially more weakly than the parent peptide (Fig. 2*B* and Table I), highlighting the important role for main chain interactions in the P5-P10 region in tight binding (45, 47). Phen7 and Min4 have similar affinity, with the decreased length of Min4 offset by its optimized side chains. The dipeptide YR exhibited very weak binding to HLA-DR1, with competition observed only at the highest concentrations tested (Fig. 2*B*).

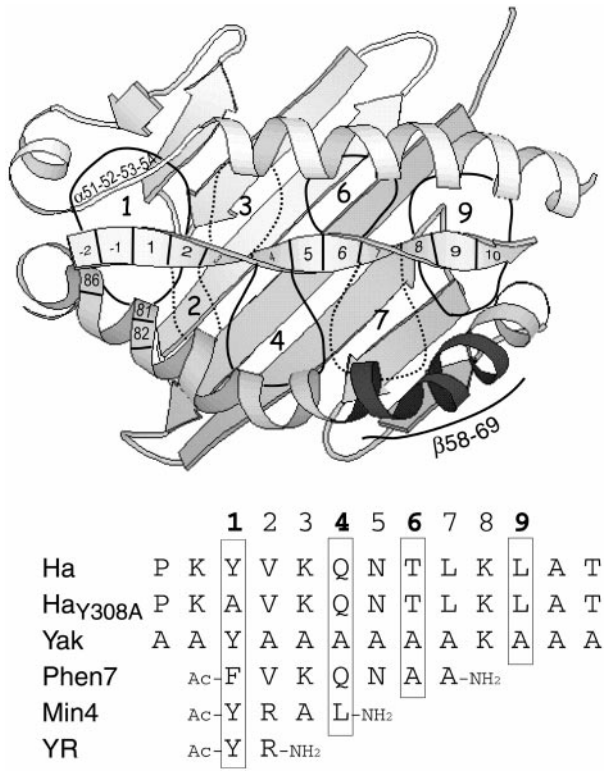

FIG. 1. **The HLA-DR1 peptide-binding site.** *Top*, ribbon diagram of the MHC class II peptide-binding site derived from the crystal structure of HLA-DR1 bound to Ha peptide, with the α subunit helical region and β strands at the *top* and *left* (*lighter ribbon*) and the β subunit helical region and β strands at the *bottom* and *right* (*darker ribbon*) (10). The region β58–69 is indicated by a *shaded ribbon*; this is the epitope for the antibody KL-295. The *twisted strand* running horizontally through the binding site is the peptide, with residue numbers indicated on the ribbon. Peptide positions −2 through 10 make extensive, conserved contacts with the MHC protein (7). *Enclosed numbered regions* indicate parts of HLA-DR1 that can be contacted by side chains of the bound peptide and correspond to the major pockets P1, P4, P6, and P9 (*solid outlines*) and the minor contact regions P2, P3, and P7 (*dotted outlines*). Peptide side chains at positions 5 and 8 are not expected to contact the MHC protein. The position of Glyβ^{86}, site of the Gβ86Y mutation introduced to partially fill the P1 pocket, and residues Hisβ^{81} and Asnβ^{82} are indicated along the β subunit helix. Residues α51–54 are indicated along an extended region on the α subunit helical region. These residues were shown to be key in the maintaining the stability of peptide-MHC complex. *Bottom*, the sequences of the peptides used in this study. *Boxes* enclose peptide residues with side chains expected to bind into pockets in the peptide-binding sites, numbered as in the *top panel*.

In previous studies, the stability of MHC-peptide complexes to SDS-induced $\alpha\beta$ chain dissociation at room temperature has been used to characterize peptide binding (33, 34, 48). We examined the stability of the peptide complexes to SDS-induced dissociation (Fig. 2*C*). Of the peptide complexes tested, only the Ha and Yak complexes were fully resistant to SDS (Fig. 2*C*). These results reiterate the point that not all peptide complexes are SDS-stable and that SDS-stability can be altered by small changes in the peptide sequence (33, 49).

Peptide Analogues All Induce Conversion to the Compact Conformation—HLA-DR1 undergoes a defined conformational change upon binding peptide, which can be observed experimentally as a decrease in hydrodynamic radius from ~35 Å for the empty protein to ~29 Å for the peptide complex (21). We tested the Ha peptide analogues for their ability to induce this conformational change using a gel filtration assay. Complexes of each of the peptide analogues exhibited decreased apparent

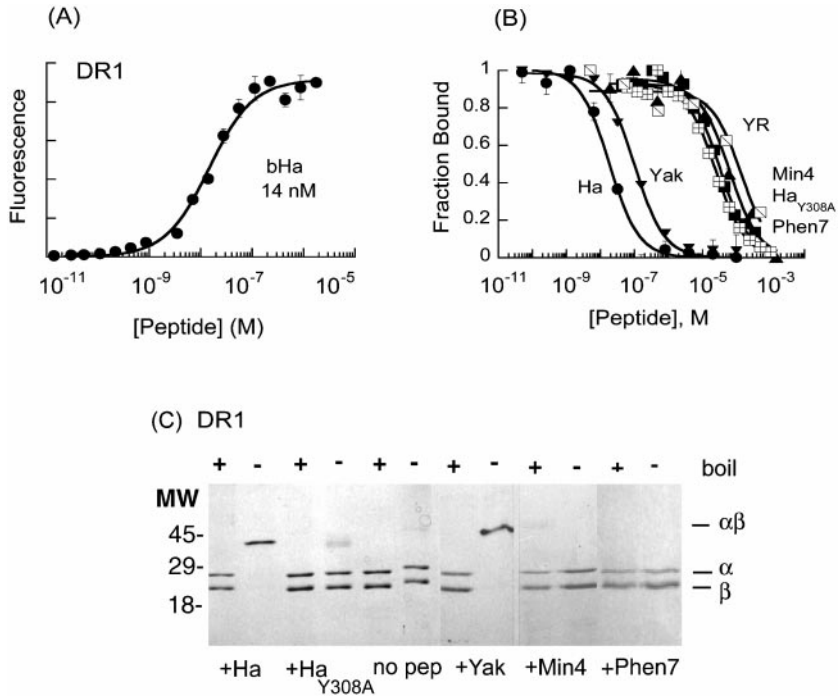

FIG. 2. **HLA-DR1-peptide complexes.** *A*, representative direct binding assay for biotinylated Ha peptide (*bHa*) with binding detected by sandwich fluorescence immunoassay. The K_D was determined by fitting to the quadratic binding equation as described under "Experimental Procedures." *B*, representative competitive binding assay for the peptides used in this study, with unlabeled peptides Ha (*closed circles*), Yak (*closed inverted triangles*), HaY308A (*open crossed squares*), Phen7 (*closed squares*), Min 4 (*closed triangles*), and YR (*slashed squares*) competing for binding with labeled bHa peptide. *Curves* represent the fits to the competitive binding equation as described under "Experimental Procedures." Average peptide binding affinities for these peptides are listed in Table I. *C*, SDS-PAGE of empty DR1 and complexes with peptides Ha, Ha_{Y308A}, Yak, Min4, and Phen7. Gels were run under reducing conditions with 12.5% acrylamide, and samples were boiled or not prior to loading as indicated, with proteins detected by staining with Coomassie Brilliant Blue R-250. Only Ha and Yak peptides conferred SDS resistance to the $\alpha\beta$ DR1 heterodimer.

TABLE I
Hydrodynamic properties of HLA-DR1 and peptide complexes

K_B, dissociation constant (from data in Figs. 2 and 6); MW_{app}, molecular weight determined by gel filtration in (Fig. 3) (×1000); D, diffusion coefficient; R_{hydr}, hydrodynamic radius; f/f_o, frictional coefficient; ND, not determined due to instability of the complex.

MHC protein	Peptide	K_D	MW_{app}	Dynamic light scattering		
				D	R_{hydr}	f/f_o
		nM		*10^{-7} cm^2/s*	*angstrom*	
DR1	none		48 ± 3	6.34 ± 0.16	34 ± 1	1.3 ± 0.04
	Ha	14	40 ± 2	7.55 ± 0.05	28 ± 2	1.0 ± 0.07
	Yak	118	41 ± 2	7.76 ± 0.40	28 ± 1	1.0 ± 0.05
	Ha_{Y308A}	23,000	38 ± 3	7.24 ± 0.18	27 ± 1	1.1 ± 0.04
	Phen7	19,000	38 ± 3	7.20 ± 0.60	30 ± 2	1.1 ± 0.09
	Min4	21,000	39 ± 2	ND	ND	ND
	YR	200,000	39 ± 2	ND	ND	ND
$DR1_{\beta G86Y}$	none		38 ± 3	ND	ND	ND
	Ha_{Y308A}	9,000	38 ± 3	7.20 ± 0.26	30 ± 1	1.1 ± 0.04

molecular weight and sharpened elution profile relative to the empty protein (Fig. 3). In each case the changes were very similar to those induced by the unmodified Ha peptide. Apparent molecular weights that were calculated from the gel filtration elution volumes are shown in Table I; the differences in MW_{app} among peptide complexes are within experimental error, but a significant difference is apparent between the MW_{app} of empty DR1 and that of the peptide complexes. A decrease in apparent molecular weight correlates to a decrease in hydrodynamic radius because both forms of the MHC are known to have essentially the same actual molecular weight. This apparent decrease in hydrodynamic radius upon peptide binding was confirmed for most of the complexes using dynamic light scattering (Table I). Thus each of the peptide analogues was able to trigger HLA-DR1 conversion to the compact conformation.

Previously, the hydrodynamic change was shown to correlate to a decrease in reactivity with the monoclonal antibody KL-295 (43). This antibody was raised against a peptide epitope on the class II β subunit helical region (Fig. 1). In complexes with Ha and other peptides, the KL-295 epitope becomes inaccessible (21). We tested HLA-DR1 complexes with each of the peptide analogues for its reactivity with KL-295. None of the complexes with the Ha analogue peptides were recognized by KL-295 (Fig. 4*A*), indicating that in each case the epitope β58–69 is made inaccessible to the antibody by the conformational shift, because

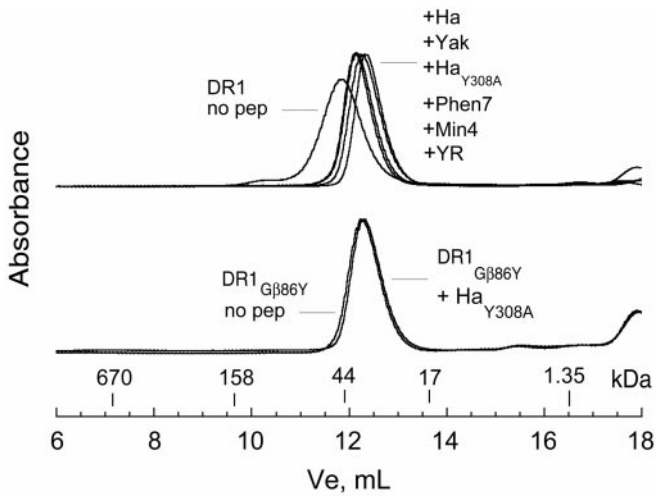

FIG. 3. **Gel filtration of empty HLA-DR1 and peptide complexes.** *Top*, wild-type HLA-DR1 and peptide complexes. *Bottom*, mutant $DR1_{G\beta86Y}$ and Ha_{Y308A} peptide complex. Peptide binding to wild-type DR1 induces conversion to a more compact form as evidenced by the larger elution volume and lower apparent molecular weight for each of the complexes, whereas the mutant $DR1_{G\beta86Y}$ exhibits a compact form for both the empty protein and the complex with the Ha_{Y308A} peptide. Derived apparent molecular weights are given in Table I.

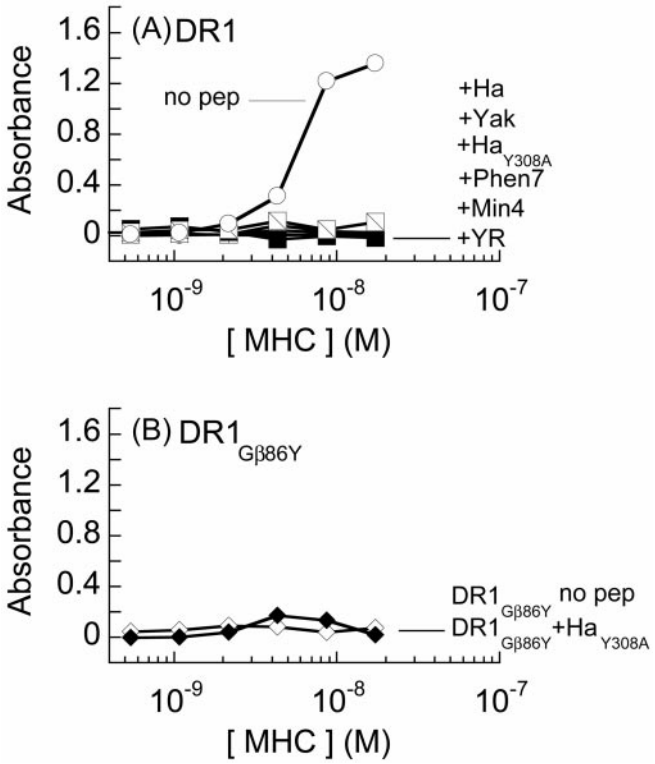

FIG. 4. **Reactivity of HLA-DR1 and peptide complexes with the conformation-specific monoclonal antibody KL-295.** Sandwich enzyme-linked immunosorbent assay using KL-295 to detect binding to complexes in the DR1 "open" conformation. *A*, KL-295 binds empty HLA-DR1 (*open circles*) but does not bind HLA-DR1 in complex with Ha (*closed circles*), Yak (*closed inverted triangles*), HaY308A (*open crossed squares*), Phen7 (*closed squares*), Min 4 (*closed triangles*), and YR (*slashed squares*). *B*, KL-295 shows no significant reactivity with monomeric $DR1_{G\beta86Y}$ either empty (*open diamonds*) or in complex with Ha_{Y308A} (*closed diamonds*).

it is in the complex with the unmodified Ha peptide.

The peptide-induced conversion to a compact form has also been correlated with an increase in cooperativity of denaturation (21), indicating that condensation of the protein around the bound peptide is accompanied by an increase in the number of stabilizing intra-protein interactions. We measured thermal denaturation profiles for complexes of each of the peptide analogues (Fig. 5). Melting temperatures for these complexes varied from 67 to 89 °C (Table II). Each of the complexes exhibited a steep denaturation profile, indicative of cooperative denaturation (Fig. 5). To compare the slope of the curve at different temperatures, the thermodynamic parameter ΔH, which primarily determines the slope of the transition, was derived from each of the denaturation traces (see "Experimental Procedures"). The values for each complex are given in Table II.

The Mutant $DR1_{G86Y}$ Has a More Compact Conformation—The results with Min4 and YR suggested that features required for induction of the hydrodynamic collapse might be localized to a relatively small region of the peptide-binding groove. The P1 pocket is known from binding and structural work to contain many important MHC-peptide contacts and appeared to be a likely site for interactions involved in triggering the hydrodynamic change. P1 is the largest and most hydrophobic of the DR1 peptide side chain binding pockets (10) and the site of $\alpha\beta$ subunit contacts and upper-lower domain contacts (7). Most of the residues lining this site (Fig. 6*A*) are highly conserved, but Valβ^{85} and Glyβ^{86} are polymorphic (50). Examination of the crystal structures of HLA-DR1 (Valβ^{85} and Glyβ^{86}) and the mouse homologue H-2Ek (Ileβ^{85} and Pheβ^{86}) suggested that the substitution of HLA-DR1 Glyβ^{86} with an aromatic group would allow an aromatic side chain in a common rotamer to fill the P1 pocket (Fig. 6*A*). Tyrosine was chosen to replace HLA-DR1 Glyβ^{86}, because its exposed ring hydroxyl group would be expected to provide a relatively hydrophilic cover for the pocket. (Fig. 6*A*) (33). The $HLA\text{-}DR1_{G\beta86Y}$ mutant protein has been previously investigated in a study of peptide binding kinetics and SDS stability (33). In the present study, the β subunit of $HLA\text{-}DR1_{G\beta86Y}$ was expressed in *E. coli* inclusion bodies and folded *in vitro* with wild-type α subunit using conditions established for the wild-type protein. The folded peptide-free $HLA\text{-}DR1_{G\beta86Y}$ protein was partially resistant to SDS-induced chain dissociation (Fig. 6*B*), somewhat less than previously observed for a similar protein produced by secretion from baculovirus-infected insect cells (33).

Empty $HLA\text{-}DR1_{G\beta86Y}$ consistently exhibited a more compact monomeric form than empty DR1, as judged by gel filtration (Fig. 3), with apparent molecular weight nearly that of peptide complexes of the wild-type protein. However, dynamic light scattering experiments indicated that the $DR1_{G\beta86Y}$ compact conformation was unstable (not shown), with a tendency to aggregate (Table I). KL-295 reacted variably with the mutated protein in that monomeric $DR1_{G\beta86Y}$ did not react with KL-295 (Fig. 4*B*), but aggregated $DR1_{G\beta86Y}$ did (not shown). This indicates that the mutation may only partially stabilize the compact conformation, which is resistant to aggregation, in an equilibrium with the open conformation, which tends to aggregate. No such reactivity differences were seen between monomeric and aggregated wild-type empty DR1. The mutant $HLA\text{-}DR1_{G\beta86Y}$ also showed a high degree of cooperativity in thermal denaturation experiments, similar to that observed for peptide complexes of the wild-type protein (Fig. 5). These results suggest that the $HLA\text{-}DR1_{G\beta86Y}$ mutant protein in its empty form can attain a compact conformation similar to that observed for peptide complexes of the wild-type protein, although it appears to lack some stabilizing interactions present in peptide complexes of HLA-DR1.

Peptide Complexes of $HLA\text{-}DR1_{G\beta86Y}$—The peptide binding activity of mutant $HLA\text{-}DR1_{G\beta86Y}$ was investigated using direct binding assays with biotinylated peptides. In complex with the mutant $HLA\text{-}DR1_{G\beta86Y}$, the Ha_{Y308A} peptide would be expected to place the Ala^{308} side chain against the P1 pocket filled by the Gβ86Y substitution, whereas peptides with large P1 residues would not be expected to bind because of steric blockage of the P1 pocket. $HLA\text{-}DR1_{G\beta86Y}$ bound the peptide Ha_{Y308A} with $K_D \sim 9\ \mu M$, similar to the value observed for this peptide binding to the wild-type protein ($K_D \sim 23\ \mu M$). On the other hand, the unmodified Ha peptide, with tyrosine at P1, bound $HLA\text{-}DR1_{G\beta86Y}$ with almost 1000-fold weaker affinity (Fig. 6*C*). The results show that the Gβ86Y substitution has the desired effect in filling the P1 pocket. $HLA\text{-}DR1_{G\beta86Y}$ bound to Ha_{Y308A} exhibits the compact monomeric conformation (Fig. 3 and Table I) and does not react with KL295 (Fig. 4*B*). Both empty $HLA\text{-}DR1_{G\beta86Y}$ and $HLA\text{-}DR1_{G\beta86Y}$ loaded with Ha_{Y308A} exhibit cooperative thermal denaturation profiles. Ha_{Y308A} binding substantially increases the denaturation midpoint temperature of $HLA\text{-}DR1_{G\beta86Y}$ relative to the empty form, showing that stabilizing interactions are formed outside the P1 region (Fig. 5 and Table II). These results show that although simple occupancy of the P1 pocket in the mutant $HLA\text{-}DR1_{G\beta86Y}$ can cause partial conversion to a compact form, additional interactions outside P1 are necessary to stabilize the compact conformation.

Both P1 Occupancy and Main Chain Interactions Are Required to Attain the Final Conformation—In previous work with HLA-DR1, the transition to a compact form concurrent

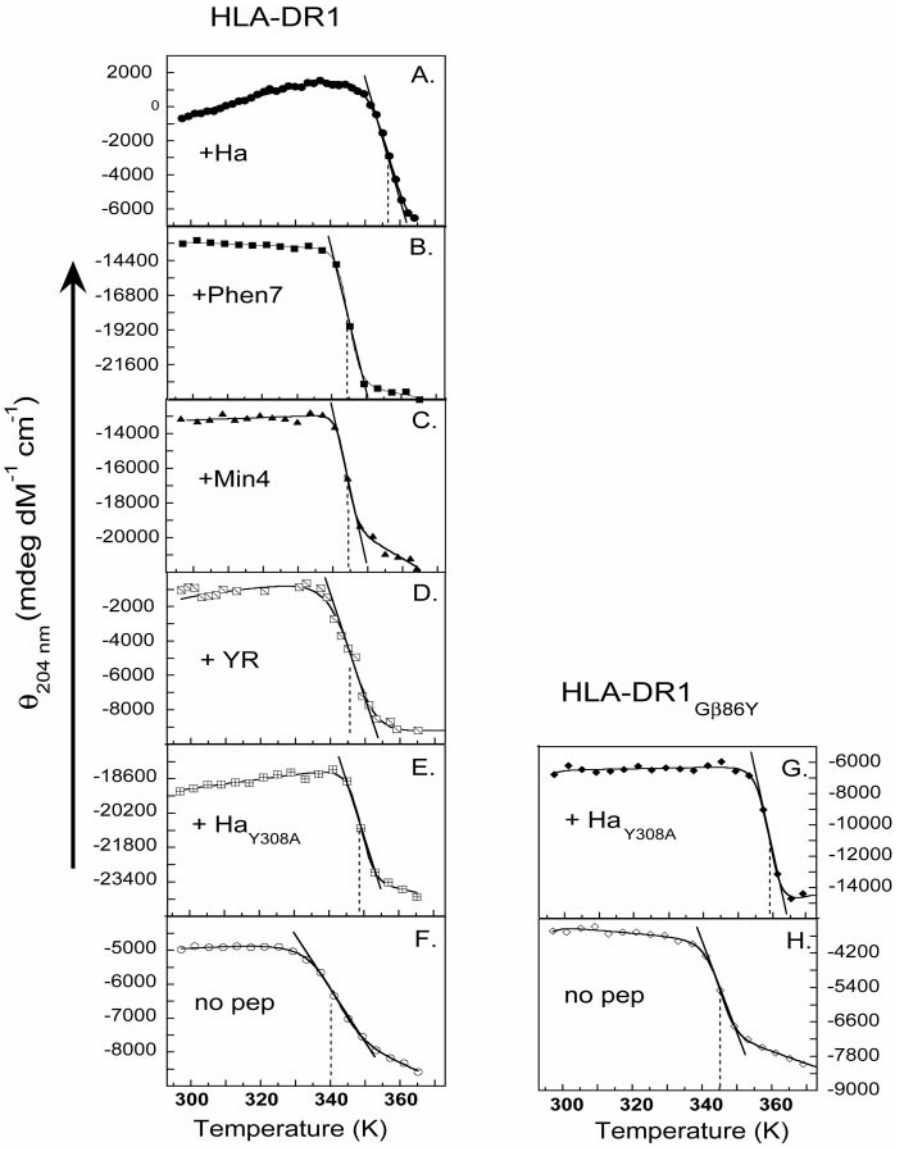

FIG. 5. **Thermal stability profiles of empty and peptide-loaded HLA-DR1 and DR1$_{G\beta86Y}$.** Thermal denaturation was followed as the change in molar ellipticity at 204 nm for HLA-DR1 in complex with Ha (*A*, *closed circles*), Phen7 (*B*, *closed squares*), Min 4 (*C*, *closed triangles*), YR (*D*, *slashed squares*), HaY308A (*E*, *open crossed squares*), and no peptide (*F*, *open circles*), as well as for DR1$_{G\beta86Y}$ in complex with Ha$_{Y308A}$ (*G*, *closed diamonds*) and no peptide (*H*, *open diamonds*). The *curves* represent the fit to a six-parameter function describing the denaturation profile as described under "Experimental Procedures." Derived parameters are shown in Table II. The midpoint of the transition is denoted with a *dotted line*.

TABLE II
Thermal stability of HLA-DR1 and peptide complexes

T_m, midpoint temperature; ΔH, changes in enthalpy at the midpoint (determined from Fig. 5).

MHC protein	Peptide	T_m	ΔH
		°C (K)	*kcal/mol*
DR1	none	67 (340)	50 ± 3
	Ha	84 (357)	72 ± 5
	Yak	89 (362)	87 ± 5
	Phen7	72 (345)	148 ± 11
	Min4	71 (344)	148 ± 22
	YR	73 (346)	71 ± 10
	Ha$_{Y308A}$	76 (349)	142 ± 17
DR1$_{\beta G86Y}$	none	72 (345)	92 ± 9
	Ha$_{Y308A}$	86 (359)	130 ± 13

with peptide binding was accompanied by small changes in the far-UV circular dichroism spectra (21). These spectral changes suggested that peptide binding induced relatively small alterations in secondary structure on the scale of conversion of ~10 residues from a disordered structure to regular conformation. We investigated whether the peptide analogues and the Gβ86Y mutation were able to effect the CD spectral change. With the wild-type protein, all of the peptide analogues that contained an aromatic group at P1, including the minimal YR peptide (Fig. 7*A*), were able to cause complete conversion of the CD spectrum to the peptide-bound form. In contrast, Ha$_{Y308A}$ induced smaller but significant changes to the CD spectrum that appeared to be consistent with partial conversion to the peptide-bound form (Fig. 7*A*). For HLA-DR1$_{G\beta86Y}$, the CD spectrum of the empty protein was most similar to that for the empty wild-type protein (Fig. 7*B*) but with increased intensity and clearly distinct from that of the empty wild-type conformation. Upon binding HLA-DR1$_{G\beta86Y}$, Ha$_{Y308A}$ induced large changes in the CD spectrum and essentially complete conversion to the peptide-bound form, as observed for the wild-type protein with Ha peptide (Fig. 7*B*). Thus of the compact, cooperatively melting, KL-295-resistant forms of HLA-DR1, there appear to be at least two different conformers that can be distinguished by their CD spectra, with the wild-type HLA-DR1-Ha$_{Y308A}$ peptide complex and the peptide-free mutant HLA-DR1$_{G\beta86Y}$ both exhibiting altered CD spectra relative to all of the other peptide complexes. These results show that both P1 and main chain interactions appear to be required to form the final structure.

DISCUSSION

In this study we have investigated which components of the peptide-MHC interaction are important in inducing conversion to the compact form. Binding of several minimal peptides as well as a point substitution in the empty HLA-DR1 protein

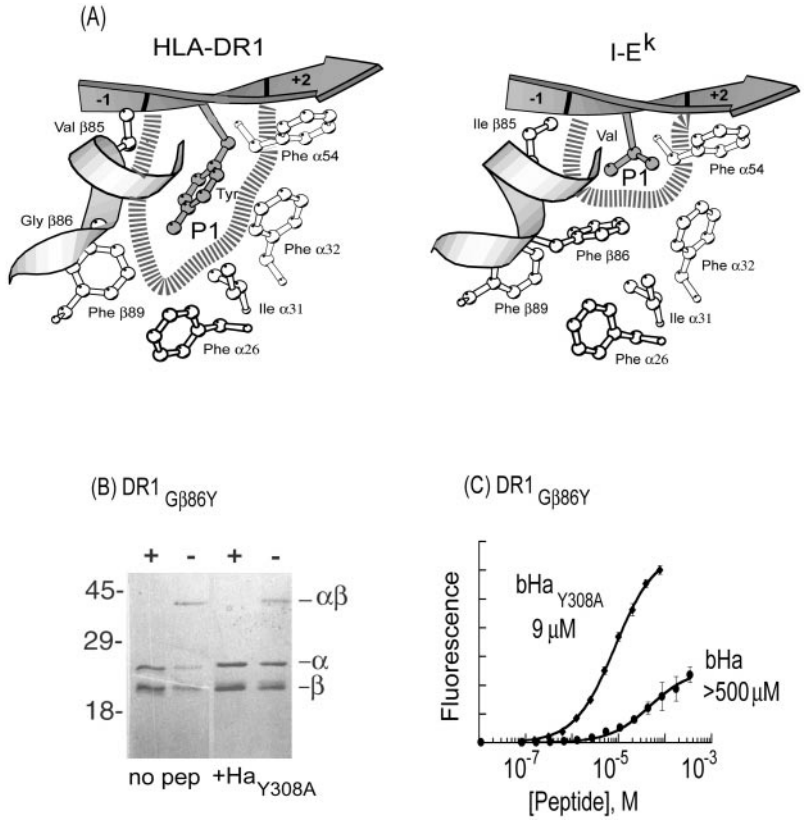

FIG. 6. **The mutant DR1$_{G\beta 86Y}$.** *A*, diagrams of the P1 pocket for HLA-DR1 and the murine homologue IE^k, drawn from the respective crystal structures (9), illustrating how the substitution of tyrosine for glycine at position β86 could partially fill the P1 pocket. The C-terminal end of the β chain helical region and all MHC residues that contact the P1 side chain are shown. The P1 pocket of HLA-DR1 is lined with hydrophobic residues and can accommodate a large, aromatic residue such as Tyr. The P1 pocket of the murine homologue of HLA-DR1, I-E^K, is nearly identical to that of HLA-DR1, except that isoleucine replaces Valβ^{85} and phenylalanine replaces Glyβ^{86}. The P1 pocket of I-E^K is shallower than that of HLA-DR1 and can only accommodate a small hydrophobic side chain. The view is rotated ~90° around a horizontal axis relative to that of Fig. 1. *B*, SDS-PAGE of HLA-DR1$_{G\beta 86Y}$ and its complex with Ha$_{Y308}$. Empty DR1$_{G\beta 86Y}$ shows a significant proportion of SDS-resistant αβ complexes, which is not increased by binding Ha$_{Y308A}$ peptide. SDS-PAGE conditions are as in Fig. 2. *C*, direct binding assay for the mutant HLA-DR1$_{G\beta 86Y}$ with biotinylated Ha$_{Y308A}$ and Ha peptides. K_D were derived as in Fig. 2 and are reported in Table I.

were shown to induce transition from an open to compact form, as measured by an 10–20% decrease in hydrodynamic radius. In each case the hydrodynamic change was accompanied by folding of a region on the β subunit corresponding to an antibody epitope and establishment of a substantial hydrophobic core exhibiting cooperative thermal denaturation. Characteristic changes in the far-UV CD spectra were observed in a subset of the compact forms. The compact conformation was stabilized by binding of peptides as short as the dipeptide YR, which binds weakly with $K_D > 100$ μM and occupies less than half of the peptide-binding cleft. Filling only the P1 pocket was sufficient to partially stabilize the compact form, as shown by the mutation HLA-DR1$_{G\beta 86Y}$. Conformational changes induced by this substitution were propagated to remote parts of the peptide-binding cleft, as indicated by loss of the KL-295 epitope in the β58–69 region at the other end of the peptide-binding site, at least 20 angstroms from the P1 region.

How does occupancy of the P1 pocket induce a conformational change in remote regions of the binding site? An attractive mechanism would involve organization of a number of aromatic side chains in the P1 pocket around the peptide P1 side chain (Fig. 6). Residues lining the pocket are from both α and β subunits, and rearrangements of these residues could be transmitted to the adjacent α and β subunit helical regions. These flanking regions are involved in important peptide main chain and side chain contacts with the MHC protein (7, 10). The conformational change involves folding or rearrangement of a part of the β chain helical region that includes at least the KL-295 epitope β58–69 (Fig. 1), and other parts of the α and β chain helical regions also may be involved. It is possible that formation of a key cluster of interactions around the P1 pocket is sufficient to nucleate a conformational change that extends throughout the peptide-binding cleft.

However, P1 occupancy was not required to induce conversion to the compact form. A variant of the Ha peptide, Ha$_{Y308A}$, was able to stabilize the compact conformation despite substitution of the P1 residue by alanine. In accordance with the model described above, the peptide Ha$_{Y308A}$ could bypass the requirement for P1 occupancy by directly contacting the α and β chain helical regions and stabilizing them in the compact form. Interestingly, neither the wild-type DR1-Ha$_{Y308A}$ complex, which lacks P1 interactions, nor the empty DR1$_{G\beta 86Y}$ protein, which lacks the other interactions, exhibited all of the features of the CD spectrum characteristic of the other peptide complexes. These proteins exhibit some of the features of a classic molten globule, *i.e.* compact tertiary structure but incomplete secondary structure.

Binding of the peptide YR is able to induce the full spectrum of effects characteristic of peptide binding. This suggests that main chain interactions in the P(−1) to P2 region are required in addition to occupancy of the P1 pocket for the complete conformational change. Main chain interactions in this region include conserved hydrogen bonding interactions between the peptide main chain at P1 and P2 and Hisβ^{81} and Asnβ^{82} side chains of DR1 and between the peptide main chain at P(−1) and P1 and α51–55 main chain atoms of DR1. The residues Hisβ^{81} (51) and Asnβ^{82} (52) have been implicated previously by mutagenesis to play a key role in stabilizing the MHC-peptide complex structure. The region α51–55 forms a conserved antiparallel β structure with the peptide N-terminal region (4–10). Interactions between these residues and the main chain of the bound peptide may comprise the set of key nucleating interactions in the P1-P4 region.

The peptide requirements for promoting conversion to the compact form of HLA-DR1 are distinct from those needed for high affinity binding. In the Ha peptide analogues, tight binding (<1 μM) requires main chain interactions in the P5–P9 region, in addition to favorable interactions in the P1–P2 pockets. In contrast, conversion to the compact form can be induced by weakly binding peptides that have P1-P2 contacts but lack P5–P9 contacts and do not contribute to the overall thermal stability of the complex. Thus Min4 and YR peptides can sta-

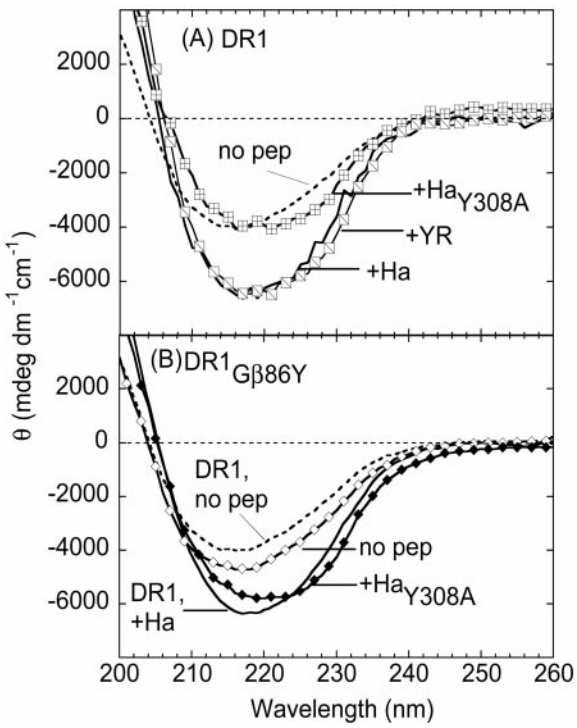

FIG. 7. **Circular dichroism spectra.** *A*, wild-type HLA-DR1, empty (*dotted line*) and in complex with peptides Ha (*solid line*), YR (*slashed squares*), and Ha_{Y308A} (*open crossed squares*). *B*, the mutant $DR1_{G\beta86Y}$, empty (*open diamonds*) and in complex with Ha_{Y308A} (*closed diamonds*). The spectra of wild-type empty HLA-DR1 (*dotted line*) and the wild-type Ha complex (*solid line*) are indicated for comparison. Both P1 occupancy with a large side chain and peptide main chain interactions are required for complete conversion to the characteristic peptide-loaded spectrum.

bilize the final structure with its characteristic CD spectrum. Ha_{Y308A}, which binds with essentially identical affinity, does not stabilize the final structure. This underscores the point that the complete set of interactions in the P1–P2 area are required for full conversion to the stable, peptide-loaded conformation, although interactions in other regions of the peptide-binding site can trigger conversion to a compact intermediate form. Thus, the interactions important for stabilizing the compact peptide-loaded conformation are different from those that stabilize the binding of the peptide, providing additional evidence that peptide binding involves rearrangement within the MHC protein and not simply creation of new MHC-peptide interactions.

A naturally occurring polymorphism in I-E, the murine homologue of HLA-DR, appears to have some of the characteristics of the $DR1_{G\beta86Y}$ protein. The k allele (I-E^k) has Pheβ^{86} (Fig. 6), as do the less frequently studied alleles I-E^p, and I-E^q (53). The hydrodynamic behavior of I-E^k has not been reported, but its cooperative thermal denaturation profile and intermediate CD spectra (23) are similar to those reported above for $DR1_{G\beta86Y}$. At pH 7, I-E^k has a lower affinity than DR1 for antigenic peptides and invariant chain, binding invariant chain with K_D ~0.3 μM and antigenic peptides with K_D values of ~0.1–10 μM (54–58), as compared with nanomolar affinities for DR1 (31, 35, 54). $DR1_{G\beta86Y}$ binds Ha_{Y308A}, a peptide expected to be optimal for this variant, with a K_D value of ~9 μM, much weaker than for typical DR1-peptide interactions but similar to those for I-E^k.

The observation that nonoverlapping sets of interactions are able to promote conversion to the compact form, as shown by the results with the Ha_{Y308A} peptide and the HLA-$DR1_{G\beta86Y}$ mutation, underscores the large scale or global nature of the conformational change. This has important implications for the mechanisms of intracellular antigen loading and transport of class II MHC proteins. MHC molecules need to form long-lived complexes with antigenic peptide to function as effective antigen-presenting elements. Release of peptide at the cell surface from short-lived complexes could allow adventitious binding of extracellular antigens, bypassing the intracellular loading pathways and possibly triggering an inappropriate immune response Moreover, several types of antigen presenting cells are known to collect antigen in peripheral tissues and transport them to lymph nodes for presentation to T-cells (59). Such cellular transport also requires long-lived MHC-peptide complexes. Experimentally, the lifetimes of MHC complexes with endogenous and antigenic peptides are quite long, on the order of hours to days (60). Kinetic studies suggest that the conformational change investigated here functions as a kinetic trap that stabilizes the bound peptide and prevents inappropriate peptide release.[2] Efficient peptide loading of class II MHC molecules *in vivo* requires the assistance of HLA-DM, a MHC homologue (62, 63) that catalyzes exchange of a bound fragment of the invariant chain chaperone for endosomal peptides (30, 31, 64–68). The mechanism for this facilitated peptide exchange remains obscure despite intensive investigation. Given the results described above, one model for DM function would be that it binds the MHC-peptide complex in the open or "noncompact" conformation. If such a species is formed transiently during the peptide binding reaction, as suggested by recent kinetic studies (20, 69),[2] interaction with DM would promote both binding and release reactions (30, 31, 61, 64, 70, 71), similar to an enzyme binding a reaction transition state. The delocalization of conformational changes around the HLA-DR1 peptide-binding site facilitates such an interaction with HLA-DM and other proteins.

In conclusion, we have shown that the association of HLA-DR1 with peptides as short as two to four residues, or partial occupancy of the P1 pocket by a point substitution, is sufficient to induce a conformational change that influences residues throughout the peptide-binding groove.

Acknowledgments—We thank Paul Travers for a helpful discussion, Danny DeOliveira for peptide synthesis, and Helen Chan for preliminary characterization of the YR, Min4, and Phen7 complexes.

REFERENCES

1. Harding, C. V. (1996) *Crit. Rev. Immunol.* **16,** 13–29
2. Germain, R. N. (1994) *Cell* **76,** 287–99
3. Brown, J. H., Jordetzky, T. S., Gorga, J. C., Stern, L. J., Urban, R. G., Strominger, J. L., and Wiley, D. C. (1993) *Nature* **364,** 33–39
4. Fremont, D. G., Monnaie, D., Nelson, C. A., Hendrickson, W. A., and Unanue, E. (1998) *Immunity* **8,** 305–317
5. Smith, K. J., Pyrdol, J., Gauthier, L., Wiley, D. C., and Wucherpfennig, K. W. (1998) *J. Exp. Med.* **188,** 1511–1520
6. Scott, C. A., Peterson, P. A., Teyton, L., and Wilson, I. A. (1998) *Immunity* **8,** 319–329
7. Murthy, V., and Stern, L. J. (1997) *Structure* **5,** 1385–1396
8. Dessen, A., Lawrence, C. M., Cupo, S., Zaller, D. M., and Wiley, D. C. (1997) *Immunity* **7,** 473–481
9. Fremont, D. H., Hendrickson, W. A., Marrack, P., and Kappler, J. (1996) *Science* **272,** 1001–1004
10. Stern, L. J., Brown, J. H., Jardetzky, T. S., Gorga, J. C., Urban, R. G., Strominger, J. L., and Wiley, D. C. (1994) *Nature* **368,** 215–221
11. Jardetzky, T. S., Brown, J. H., Gorga, J. C., Stern, L. J., Urban, R. G., Strominger, J. L., and Wiley, D. C. (1996) *Proc. Natl. Acad. Sci. U. S. A.* **93,** 734–738
12. Rammensee, H. G. (1995) *Curr. Opin. Immunol.* **7,** 85–96
13. Chicz, R. M., Urban, R. G., Lane, W. S., Gorga, J. C., Stern, L. J., Vignali, D. A. A., and Strominger, J. L. (1992) *Nature* **358,** 764–768
14. Rudensky, A., Preston-Hurlburt, P., Hong, S. C., Barlow, A., and Janeway, C. A., Jr. (1991) *Nature* **353,** 622–627
15. Hunt, D. F., Henderson, R. A., Shabanowitz, J., Sakaguchi, K., Michel, H., Sevilir, N., Cox, A. L., Appella, E., and Engelhard, V. H. (1992) *Science* **255,** 1261–1263
16. Ghosh, P., Amaya, M., Mellins, E., and Wiley, D. C. (1995) *Nature* **378,** 457–462

[2] R. Joshi, J. A. Zarutskie, and L. J. Stern, submitted for publication.

17. O'Sullivan, D., Sidney, J., Appella, E., Walker, L., Phillips, L., Colon, S., Miles, C., Chesnut, R. W., and Sette, A. (1990) *J. Immunol.* **145,** 1799–1808
18. Hammer, J., Takacs, B., and Sinigaglia, F. (1992) *J. Exp. Med.* **176,** 1007–1013
19. Sturniolo, T., Bono, E., Ding, J., Raddrizzani, L., Tuereci, O., Sahin, U., Braxenthaler, M., Gallazzi, F., Protti, M. P., Sinigaglia, F., and Hammer, J. (1999) *Nat. Biotechnol.* **17,** 555–561
20. Natarajan, S. K., Assadi, M., and Sadegh-Nasseri, S. (1999) *J. Immunol.* **162,** 4030–4036
21. Zarutskie, J. A., Sato, A. K., Rushe, M. M., Chan, I. C., Lomakin, A., Benedek, G. B., and Stern, L. J. (1999) *Biochemistry* **38,** 5878–5887
22. Rabinowitz, J. D., Vrljic, M., Kasson, P. M., Liang, M. N., Busch, R., Boniface, J. J., Davis, M. M., and McConnell, H. M. (1998) *Immunity* **9,** 699–709
23. Reich, Z., Altman, J. D., Boniface, J. J., Lyons, D. S., Kozono, H., Ogg, G., Morgan, C., and Davis, M. M. (1997) *Proc. Natl. Acad. Sci. U. S. A.* **94,** 2495–2500
24. Runnels, H. A., Moore, J. C., and Jensen, P. E. (1996) *J. Exp. Med.* **183,** 127–136
25. Boniface, J., Lyons, D., Wettstein, D., Allbritton, N., and Davis, M. M. (1996) *J. Exp. Med.* **183,** 119–126
26. Sadegh-Nasseri, S., Stern, L. J., Wiley, D. C., and Germain, R. N. (1994) *Nature* **370,** 647–650
27. Dornmair, K., Rothenhausler, B., and McConnell, H. M. (1989) *Cold Spring Harbor Symp. Quant. Biol.* LIV 409–416
28. Dornmair, K., and McConnell, H. M. (1990) *Proc. Natl. Acad. Sci. U. S. A.* **87,** 4134–4138
29. Sadegh-Nasseri, S., and Germain, R. N. (1991) *Nature* **353,** 167–170
30. Denzin, L. K., and Cresswell, P. (1995) *Cell* **82,** 155–165
31. Kropshofer, H., Vogt, A. B., Moldenhauer, G., Hammer, J., Blum, J. S., and Hammerling, G. J. (1996) *EMBO J.* **15,** 6144–6154
32. Frayser, M., Sato, A. K., Xu, L., and Stern, L. J. (1999) *Protein Expression Purif.* **15,** 105–114
33. Natarajan, S. K., Stern, L. J., and Sadegh-Nasseri, S. (1999) *J. Immunol.* **162,** 3463–3470
34. Stern, L. J., and Wiley, D. C. (1992) *Cell* **68,** 465–477
35. Roche, P. A., and Cresswell, P. (1990) *J. Immunol.* **144,** 1849–1856
36. Jensen, P. E., Moore, J. C., and Lukacher, A. E. (1998) *J. Immunol. Methods* **215,** 71–80
37. Siegel, L. M., and Monty, K. J. (1966) *Biochim. Biophys. Acta* **112,** 346–362
38. Asherie, N., Pande, J., Lomakin, A., Ogun, O., Hanson, S. R., Smith, J. B., and Benedek, G. B. (1998) *Biophys Chem* **75,** 213–227
39. Cantor, C. R., and Schimmel, P. R. (1980) *Biophysical Chemistry*, Vol. II, W. H. Freeman and Company, New York
40. Privalov, P. L., and Gill, S. J. (1988) *Adv. Protein Chem.* **39,** 193–234
41. Becktel, J., and Schellman, J. A. (1987) *Biopolymers* **26,** 1859–1877
42. Sanchez-Ruiz, J. M. (1992) *Biophys. J.* **61,** 921–935
43. Lapan, K. L., Klapper, D. G., and Frelinger, J. A. (1992) *Hybridoma* **11,** 217–223
44. Jardetzky, T. S., Gorga, J. C., Busch, R., Rothbard, J., Strominger, J. L., and Wiley, D. C. (1990) *EMBO J.* **9,** 1797–1803
45. Hammer, J., Belunis, C., Bolin, D., Papdopoulos, J., Walsky, R., Higelin, J., Danho, W., Sinigaglia, F., and Nagy, Z. A. (1994) *Proc. Natl. Acad. Sci. U. S. A.* **91,** 4456–4460
46. Hammer, J., Bono, E., Gallazzi, F., Belunis, C., Nagy, Z., and Sinigaglia, F. (1994) *J. Exp. Med.* **180,** 2353–2358
47. O'Sullivan, D., Sidney, J., del Guercio, M.-F., Colon, S., and Sette, A. (1990) *J. Immunol.* **146,** 1240–1246
48. Wu, S., Gorski, J., Eckels, D. D., and Newton-Nash, D. K. (1996) *J. Immunol.* **156,** 3815–3820
49. Nelson, C. A., Petzold, S. J., and Unanue, E. R. (1993) *Proc. Natl. Acad. Sci. U. S. A.* **90,** 1227–1231
50. Newton-Nash, D. K., and Eckels, D. D. (1993) *J. Immunol.* **150,** 1813–1821
51. Tan, L. J., Ceman, S., Chervonsky, A., Rodriguez-Paris, J., Steck, T. L., and Sant, A. J. (1997) *Eur. J. Immunol.* **27,** 1479–1488
52. Griffith, I. J., Nabavi, N., Ghogawala, Z., Chase, C. G., Rodriguez, M., McKean, D. J., and Glimcher, L. H. (1988) *J. Exp. Med.* **167,** 541–555
53. Rammensee, H.-G. (1997) *MHC Ligands and Peptide Motifs*, Chapman & Hall, Landes Bioscience, Austin, TX
54. Sette, A., Southwood, S., Miller, J., and Appella, E. (1995) *J. Exp. Med.* **181,** 677–683
55. Reay, P., Wettstein, D. A., and Davis, M. M. (1992) *EMBO J.* **11,** 2829–2839
56. Leighton, J., Sette, A., Sidney, J., Appella, E., Ehrhardt, C., Fuchs, S., and Adorini, L. (1991) *J. Immunol.* **147,** 198–204
57. Buus, S., Sette, A., Colon, S., Miles, C., and Grey, H. M. (1987) *Science* **235,** 1353–1358
58. Sadegh-Nasseri, S., and McConnell, H. M. (1989) *Nature* **337,** 274–276
59. Banchereaur, J., and Steinman, R. M. (1998) *Nature* **392,** 245–252
60. Lanzavecchia, A., Reid, P. A., and Watts, C. (1992) *Nature* **357,** 249–252
61. Sloan, V. S., Cameron, P., Porter, G., Gammon, M., Amaya, M., Mellins, E., and Zaller, D. M. (1995) *Nature* **375,** 802–806
62. Fremont, D. H., Crawford, F., Marrack, P., Hendrickson, W. A., and Kappler, J. (1998) *Immunity* **9,** 385–393
63. Mosyak, L., Zaller, D. M., and Wiley, D. C. (1998) *Immunity* **9,** 377–383
64. Sherman, M. A., Weber, D. A., and Jensen, P. E. (1995) *Cell* **3,** 197–205
65. Stebbins, C. C., Peterson, M. E., Suh, W. M., and Sant, A. J. (1996) *J. Immunol.* **157,** 4892–4898
66. van Ham, S. M., Gruneberg, U., Malcherek, G., Broker, I., Melms, A., and Trowsdale, J. (1996) *J. Exp. Med.* **184,** 2019–2024
67. Vogt, A. B., Kropshofer, H., Moldenhauer, G., and Hammerling, G. J. (1996) *Proc. Natl. Acad. Sci. U. S. A.* **93,** 9724–9729
68. Weber, D., Evavold, B. D., and Jensen, P. E. (1996) *Science* **274,** 618–620
69. Rabinowitz, J. D., Liang, M. N., Tate, K., Lee, C., Beeson, C., and McConnell, H. M. (1997) *Proc. Natl. Acad. Sci. U. S. A.* **94,** 8702–8707
70. Katz, J. F., Stebbins, C., Appella, E., and Sant, A. J. (1996) *J. Exp. Med.* **184,** 1747–1753
71. Kropshofer, H., Arndt, S. O., Moldenhauer, G., Hammerling, G. J., and Vogt, A. B. (1997) *Immunity* **6,** 293–302